Dyes and Pigments 90 (2011) 129–138

Contents lists available at ScienceDirect

Dyes and Pigments

journal homepage: www.elsevier.com/locate/dyepig

Synthesis and spectral characteristics of fluorescent dyes based on coumarin fluorophore and hindered amine stabilizer in solution and polymer matrices

Martin Danko*, Erik Szabo, Pavol Hrdlovic

Polymer Institute, Center of Excellence GLYCOMED, Slovak Academy of Sciences, 845 41 Bratislava, Dubravska cesta 9, Slovakia

ARTICLE INFO

Article history:
Received 1 October 2010
Received in revised form
8 December 2010
Accepted 9 December 2010
Available online 17 December 2010

Keywords:
Fluorescence dye
Coumarin
Sterically hindered amine
N-oxyl
Intramolecular quenching
Solvent effect

ABSTRACT

The spectral properties of novel bifunctional dyes based on – coumarin and diethylamino-coumarin and piperidine parent amine and *N*-oxyl and *N*-alkoxy derivatives were compared in cyclohexane, methanol, diethylene glycol, acetonitrile and chloroform solvents and in polystyrene, poly(methyl methacrylate) and poly(vinyl chloride) polymer matrices. The fluorescence of the derivatives excited at the longest-wavelength band around 295 nm is very low for coumarin-based dyes, whereas the fluorescence of the 7-diethylamino-3-carboxy coumarin dyes excited at 420 nm is as intense as that of anthracene in comparable conditions. Intramolecular quenching on the singlet level, monitored by fluorescence and expressed as the ratio of Φ_{NH}/Φ_{NO} for the parent amine and *N*-oxyl and Φ_{NOR}/Φ_{NO} for *N*-alkyloxy and *N*-oxyl, is more efficient in polymer matrices than in solvents. The spectral properties of 7-diethylamino-3-carboxy coumarin fluorophores depend on the polarity and viscosity of the environment. Highest values of quantum yield ratio were observed for 7-diethylamino-3-carboxy coumarin dyes in polystyrene and poly(vinylchloride). Though the fluorescence intensity is higher in chloroform or in poly(vinyl chloride) matrices, the intramolecular quenching efficiency of a given fluorophore by nitroxide is higher in low polarity media, such as cyclohexane and polystyrene.

1. Introduction

Fluorescence spectroscopy attracts considerable attention because of its sensitivity in systems containing intrinsic fluorophores and systems in which they might be introduced [1,2]. Biopolymers and synthetic polymers are used in numerous studies in which fluorescence plays an important role [2,3].

Various fluorescence probes based on fluorophores of different structures are used to monitor processes in environments such as solutions, micelles and solid amorphous matrices [4–6]. The spectral parameters of fluorescence that exhibit strong dependence on medium, such as the position of the maximum, its intensity and enhancement or quenching are exploited in these probes. The advantages of parameters connected with fluorescence are high sensitivity, simple detection and easy quantitative evaluation for selected fluorophores.

In the 1990s, a specific group of probes (dyes) was developed that are based on intramolecular fluorescence quenching. In these probes, the fluorophores are linked with a structural unit easily oxidized on the aminooxide of the *N*-oxyl type, which exhibits paramagnetic properties [7,8]. Fluorescence switch-off or switch-on occurs as a result of a chemical reaction on this reaction center.

Other fluorophores of varying complexity were tested for the construction of this probe: 1-naphthoic, 1-naphthylacetic [9], 4-(1-pyrene) alcanoic acids [10,11], 1,8-naphthaleneimide [12,13] and anthracene [14]. These fluorophores were linked with sterically hindered amines (known piperidine structure used for foto- and thermal stabilization of polymers – hindered amine stabilizers (HAS)), such as 2,2,6,6-tetramethyl-4-hydroxypiperidine, 2,2,6,6-tetramethyl-4-aminopiperidine in the form of the parent amine, nitroxyl radicals and alkoxy derivatives.

The efficiency of intramolecular quenching in these dyes depends on the size of the linker as well as on the medium. The stability of fluorophores under conditions of radical reactions is also an issue. The linkage of the above-mentioned fluorophores with sterically hindered amines does not seem to protect the fluorophore from radical (photo-oxidative) damage in the solid state [15–17].

Dyes based on intramolecular quenching that link suitable fluorophores with *N*-oxyl have been prepared and employed for various applications. Hideg and co-workers [18–20] prepared and optimized synthesis of double-sensor (fluorescent and spin) molecules with dansyl, aminophthalimide, coumarins, pyrene and 4-nitrobenzofurazan fluorophores attached to nitroxide, inspired

* Corresponding author. Tel.: +421 2 54777404; fax: +421 2 54775923.
E-mail addresses: upoldan@savba.sk (M. Danko), upolhrdl@savba.sk (P. Hrdlovic).

0143-7208/$ – see front matter © 2011 Elsevier Ltd. All rights reserved.
doi:10.1016/j.dyepig.2010.12.006

by tetramethylpiperidine or tetramethyl-2,5-dihydro-1*H*-pyrrole, which monitors reactive oxygen species in thylakoid membranes and the side-specific labeling of proteins. Dual fluorophore-nitroxide probes were used for the determination of vitamin C in biological liquids [21]. Nitroxide-linked naphthalene was used as a fluorescent dye for hydroxyl radicals [22]. A novel naphthalene-hindered amine linked with a long alkyl chain was tested as a thermo- and photo-stabilizer [23]. To gain some insight into the radical processes occurring during the induction period in the thermal degradation of polyolefins, a novel pro-fluorescent probe based on phenanthrene and diphenyl-anthracene were used [24,25].

A new approach for the detection of carbon-centered radicals in enzymatic processes was developed using pre-fluorescent dyes with quinoline as the fluorophore, which was linked with TEMPO [26]. Fluorescent imaging using a pre-fluorescent radical probe was employed for the mapping of photo-generated radicals in thin polymer films [27]. Fluorescent sensor applications, including detection of DNA damage, free radical formation and micro-lithography, have been recently reviewed [28].

Adducts of 1,8-naphthaleneimide and sterically hindered amine were used as 'one-step' brighteners and stabilizers [29].

In our laboratory, the fluorophore benzothioxanthone, which yields bright fluorescence, was used for the construction of this type of probe, and its stability in polymer matrices was recently tested [30,31].

In this study, dyes based on simple fluorophores, derivatives of coumarin and sterically hindered amine were prepared, and their spectral properties were compared in solution and in polymer matrices. A new approach for carboxyamide formation of electron-rich aromatic chromophores was employed using a triazine-based mediator. The goal of the spectroscopic study was to gain better understanding of the photophysical processes leading to intramolecular fluorescence quenching.

2. Experimental

2.1. Synthesis of dyes

The structures and preparation methods of reactants and dyes under study are shown in Schemes 1, 2 and 3. The fluorophore coumarin-3-carboxylic acid (**1**) is a commercial product (Sigma–Aldrich, Slovakia) and was used as received. The synthesis of 7-*N*,*N*-diethylaminocoumarin-3-carboxylic acid (**2**) was performed according to the synthetic details described in the work of Song et al. [37]. The linkage of fluorophores with 4-amino-2,2,6,6-tetramethylpiperidine and its *N*-oxyl and *N*-alkoxy derivatives was performed by standard organic synthesis procedures. The preparation of 4-Amino-2,2,6,6-tetramethylpiperidine-*N*-oxyl from 4-amino-2,2,6,6-tetramethylpiperidine was performed in three steps by the acetic amide protection of $-NH_2$, oxidation of piperidine nitrogen with H_2O_2 and deprotection of the amine by hydrolysis according to procedure described in Ref. [32]. For the amide formation of **1** with 4-amino-2,2,6,6-tetramethylpiperidine, a 2,6-dimethoxy-1,3,5-triazine-*N*-methylmorpholinium chloride (DMT-MM, **7**) was used as a mediator [33,34]. DMT-MM was prepared from 4-chloro-2,6-dimethoxy-1,3,5-triazine and *N*-methylmorpholine in tetrahydrofuran (THF) solution according to Ref. [35].

2.1.1. Coumarin-3-carboxy-(2,2,6,6-tetramethylpiperidine-4-yl) amide (*1a*)

Compound **1** (2 g, 10.5 mmol) was dissolved in 30 ml of commercial THF in a 100-ml round-bottomed flask. The 4-amino-2,2,6,6-tetramethyl-piperidine **4** (10% molar excess) solution in THF (20 ml) was added to this solution. A few minutes after the addition, rapid precipitation occurred in the reaction mixture. After stirring for 10 min, the dry powder of **7** (10% molar excess of **1**) was added to the reaction mixture and stirring was continued at r.t. for approx. 18 h. The reaction was followed on TLC chromatography (SiO_2 plate) using methanol as the eluent. The reaction mixture was poured into water and extracted three times with ether. The ^1H NMR analysis of the organic layer after evaporation of solution did not confirm the presence of products. The white precipitate that formed between the ether and water layers was separated by filtration and was identified as the product in the form of an amino-hydrochloride salt. The parent amine was obtained from methanol solution by the addition of 30% of ammonium hydroxide (5 ml) in 55 ml of water. The white needles that formed were filtered and dried under vacuum at 80 °C. The yield of pure product was 1.15 g (32%) of white needles with a m.p. of 190–192 °C.

^1H NMR ($CDCl_3$) δ(ppm): 1.1 (d, 2H, $-CH-\underline{CH_2}$ equatorial); 1.18 (s, 6H, $-CH_3$ equatorial); 1.31 (s, 6H, $-CH_3$ axial); 2.02 (dd, 2H,

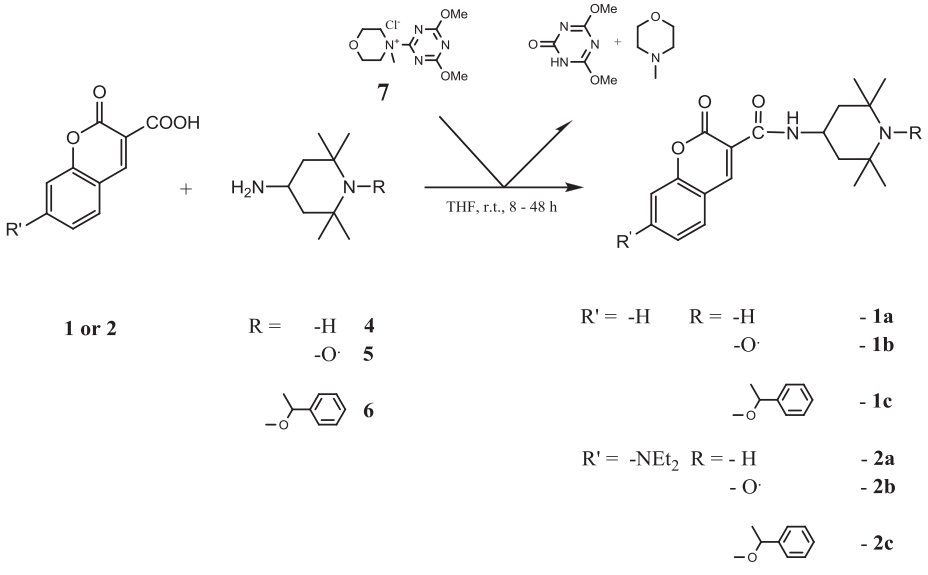

Scheme 1. The synthetic scheme for preparation of coumarin and diethylamino-coumarin derivatives (**1a**–**c** and **2a**–**c**).

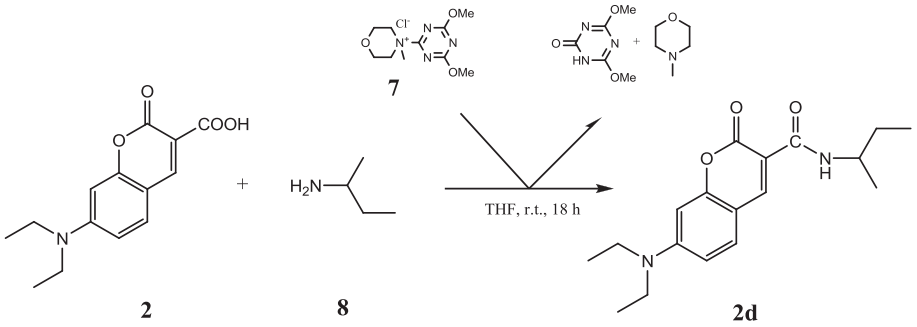

Scheme 2. The synthetic scheme for preparation of the model diethylamino-coumarin alkylamide (**2d**).

−CH−CH$_2$ axial); 4.46 (tt, 1H, −CH−); 7.37–7.45 (m, 2H, coumarin); 7.63–7.75 (m, 2H, coumarin); 8.66 (d, 1H, −NH−); 8.9 (s, 1H, >C═CH−methylene).

^{13}C NMR ($CDCl_3$) δ (ppm): 28.5 (2 × −CH_3 equat); 35.02 (2 × −CH_3 axial); 43.0 (CH−N); 45.03 (2 × CH_2−CH−N); 51.5 (C−NH); 115.4 (CH-8 coumarin); 118.1 (C-3 coumarin); 118.2 (C-10 coumarin) 125.1 (CH-6 coumarine); 129.7 (CH-5 coumarin); 133.9 (CH-7 coumarin); 148.1 (−CH═methylene); 154.6 (C-10 coumarine); 161.1 (C═O lactone); 162.2 (C═O amide).

FTIR (KBr) ν (cm^{-1}): 3435, 3318, 3050, 2960, 2925, 1705, 1659, 1612, 1569, 1546, 1456, 1364, 1248, 1161, 799, 748, 640.

Anal. Calcd. for $C_{19}H_{24}N_2O_3$: C69.49, H7.37, N8.53. Found: C69.24, H7.42, N7.75.

2.1.2. Coumarin-3-carboxy-(N-oxy-2,2,6,6-tetramethylpiperidine-4-yl)amide (*1b*)

The synthesis of **1b** was carried out using **7** as mediator, similar to **1a**. **1** (1.5 g, 7.9 mmol) reacted with 4-amino-1-oxo-2,2,6,6-tetramethylpiperidine **5** (1.49 g, 10% molar excess) and **7** (2.4 g, 10% molar excess) in THF solution. The reaction was stopped when the TLC analysis (SiO_2 plates, mixture ethylacetate/*i*-hexane 1/5 eluent) of the reaction mixture showed no signs of any further changes in its composition (~18 h). The formed precipitate was separated by filtration and thoroughly washed on the funnel with THF (6 × 15 ml), leaving the precipitate completely white and accumulating approx. 120 ml of orange filtrate. The filtrate was reduced in volume on a rotary evaporator to approx. 25 ml and cooled in the freezer. Formed orange crystals were collected by filtration and dried, yielding 2.4 g of crude product (86%). The product was recrystallized from THF, yielding pale orange crystals with a m.p. of 222–227 °C. The purity of product (100%) was confirmed by ESR analysis comparing with 4-hydroxy-1-oxy-2,2,6,6-tetramethylpiperidine in toluene solution (1 × 10^{-3} mol L^{-1}).

^{1}H NMR ($CDCl_3$, reduced by pentafluorophenyl hydrazine) δ (ppm): 1.25; (s, 6H, −CH_3 equatorial); 1.28 (s, 6H, −CH_3 axial); 1.57 (t, 2H, −CH−CH_2 equatorial); 2.01 (2H, −CH−CH_2 axial); 1.96 and 2.07 (2 strong singlets-residual pentafluorophenyl hydrazine), 3.92 (wide, 1H, >N−OH), 4.46 (m, 1H, −CH−); 5.11 (wide singlet - residual pentafluorophenyl hydrazine); 6.38 (wide singlet - residual pentafluorophenyl hydrazine); 7.36–7.46 (m, 2H, coumarin); 7.63–7.76 (m, 2H, coumarin); 8.66 (d, 1H, −NH−); 8.9 (s, 1H, >C═CH−methylene).

FTIR (KBr) ν (cm^{-1}): 3454, 3322, 2972, 2940, 1696, 1652, 1619, 1589, 1532, 1516, 1417, 1355, 1232, 1192, 1134, 1079, 792, 700.

2.1.3. 4-Amino-1-(1′-phenylethyl)oxy-2,2,6,6-tetramethylpiperidine (*6*)

The protection and deprotection of the amino group was performed according to the method described in Ref. [36] by di-*tert*-butyldicarbonate (Boc_2O) and hydrolysis with tri-fluoro-acetic acid (CF_3COOH).

Three molar equivalents of $NaHCO_3$ and a 20% molar excess of Boc_2O were consecutively added to the stirred solution of **5** (1 g, 5.85 mmol) in a THF/water mixture (1/1, 60 ml) in portions at 0 °C over 45 min. The reaction mixture was then stirred overnight at r.t. The solution was then extracted with three portion of ether, and the organic phases were washed with water and dried over Na_2SO_4. After the evaporation of ether and drying, that formed orange needles (1.5 g, 95%) were used further reaction.

The protected *N*-oxyl (BOC-NO, 1.5 g, 5.53 mmol) was dissolved in a 150-ml mixture of toluene/ethanol (1/1), and a ten-fold molar excess of styrene (5.1 g, freshly distilled) and $Mn(OAc)_3\,2H_2O$ (14.8 g) were added to the solution. The mixture was stirred in an open 250-ml round-bottomed flask. Three loads of $NaBH_4$ (15-fold molar excess with respect to BOC-NO, 3.15 g) were added portionwise in 15-min intervals to avoid the boiling of the reaction mixture. After

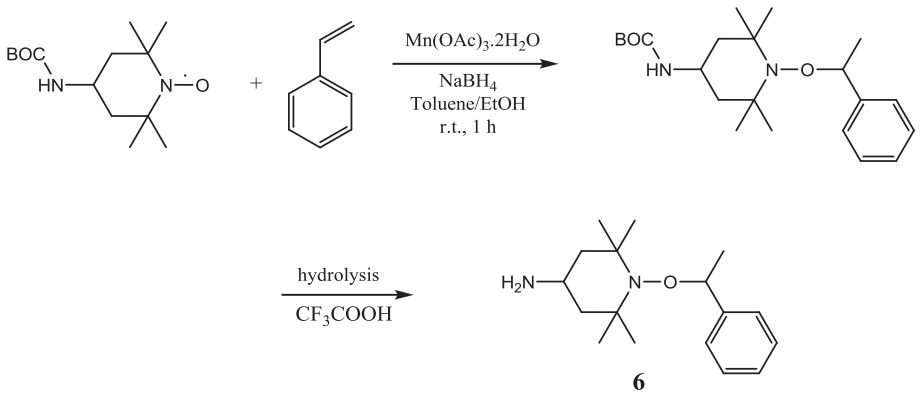

Scheme 3. The synthetic scheme for the preparation of the 4-amino-2,2,6,6-tetramethylpiperidine-*N*-alkoxyamine *via* protection and deprotection of the free amino group.

the filtration of the inorganics, the solvents were evaporated and the product was separated on a silica column using *i*-hexane/ethylacetate (5/1, v/v) as the eluent, yielding 1.56 g (75%) of white powder.

BOC-NOR (1.55 g) was treated with CF_3COOH (8 ml, 26 molar excess) in dichloromethane at r.t. for the deprotection of amine. Product **6** was formed as a white precipitate after the addition of a water solution of $NaHCO_3$ to the reaction mixture and was separated by filtration (yield 1.01 g, 89%). FTIR analysis (KBr pellet) of the washed and dried white powder did not show carboxyamide absorption. For further reactions, **6** was used as the crude product.

All protection, N-oxyl formation and deprotection products were analyzed by FTIR analysis in chloroform solution.

2.1.4. Coumarin-3-carboxy-(1-(1′-phenylethyl)oxy-2,2,6,6-tetramethylpiperidine-4-yl)amide (**1c**)

The synthesis of **1c** was carried out using mediator **7**, similar to that of **1b**. **1** (0.63 g, 3.3 mmol), reacted with **6** (1.01 g, 10% molar excess) and **7** (1.01 g, 10% molar excess) in THF solution. Because only small changes were observed using TLC analysis SiO_2 plate, elution ethylacetate/*i*-hexane (1/5, v/v) of the reaction mixture stirred at r.t., the reaction was continued at 55 °C for 8 h. The formed precipitate was separated by filtration and thoroughly washed on the funnel with THF (6 × 10 ml). The solvent was evaporated on a rotary evaporator, and the solid residue was separated (chromatographed) on the silica column using gradient elution of ethylacetate/*i*-hexane mixtures, starting with a 1/5 mixture and finishing with pure ethylacetate. Only the last fraction was identified by NMR analysis as a product; preceding fractions did not contain NMR signals related to the coumarin fluorophore. The yield of coumarin − *N*-alkoxyamine was 28% of theoretical amount of small white crystals with a m.p. of <120 °C (carbonization).

^{1}H NMR ($CDCl_3$) δ(ppm): 0.68 (s, 3H, 1 × CH_3 equatorial); 1.17 (s, 6H, 1 × CH_3 equatorial); 1.32–1.35 (2 × s, 6H, 2 × $-CH_3$ axial); 1.5 (d, 3H, −CH−$\underline{CH_3}$, J = 6.68 Hz); 1.57 (t, 2H, −CH−$\underline{CH_2}$ equatorial); 1.80 (td, 1H, −$\overline{CH}$−$\underline{CH_2}$ axial); 1.93 (td, 1H, −CH−CH_2 axial); 4.31 (m, 1H, −$\underline{CH}$−NH−); 4.79 (q, 1H, −$\underline{CH}$−CH_3, J = 6.68 Hz) 7.20–7.32 (m, 5H, 1-Phenyl); 7.34–7.43 (m, 2H, coumarin); 7.62–7.72 (m, 2H, coumarin); 8.59 (d, 1H, −$\underline{NH}$−CH−); 8.87 (s, 1H, >C=$\underline{CH}$−methylene).

^{13}C NMR ($CDCl_3$) δ(ppm): 20.9 ($\underline{CH_3}$−CH−Ph); 23.3 (CH_3 axial); 30.9 (>$\underline{CH}$−CH_3); 34.0 and 34.3 ($\overline{CH_3}$ equat.); 41.7 (CH−NH); 45.9 ($\underline{CH_2}$−$\overline{CH}$−N); 59.8 and 60.1 (2 × C−N); 83.3 (CH_3−$\underline{CH}$−Ph); 116.6 ($\overline{CH}$-8 coumarin); 118.6 (C-3 lactone); 118.7 (C-10 coumarin); 125.2 (CH-6 coumarin); 126.7 (CH-2,6 phenyl); 126.9 (CH-4 phenyl); 128.0 (CH-3,5 phenyl); 129.8 (C-5 coumarin); 133.9 (−CH=methylene); 145.4 (C-1 phenyl); 148.1 (C-7 coumarin); 154.4 (C-9 coumarin); 160.7 (C=O lactone); 161.4 (C=O amide).

FTIR (KBr) ν (cm^{-1}): 3451, 3328, 2974, 2934, 1714, 1655, 1613, 1570, 1539, 1457, 1365, 1241, 1078, 948, 799, 759, 699, 633.

Anal. Calcd. for $C_{27}H_{32}N_2O_4$: 72.30, H7.19, N6.25. Found: C72.18, H7.22, N5.44.

2.1.5. 7-N,N-diethylaminocoumarin-3-carboxylic acid (**2**)

Product **2** was prepared according to the procedure of Song et al. [37] in 63% yield. The product was crystallized from the reaction mixture after cooling to −25 °C as orange crystals with a m.p. of 230–232 °C (ref. [37] m.p. 222–224 °C) and was used for next step without further purification. The chemical structure and purity of this compound were proven by ^{1}H NMR.

2.1.6. 7-(N,N-diethylamino)coumarin-3-carboxy-(2,2,6,6-tetramethylpiperidine-4-yl)amide (**2a**)

The synthesis of **2a** was performed as for **1a**, using compounds **2** (1.16 mmol), **4** (1.27 mmol) and **7** (1.27 mmol) in THF solution for 18 h. The product was crystallized from the reaction mixture as a hydrochloride salt. Another portion of the product was formed during the evaporation of the THF solvent from the reaction mixture. The pure parent amine was separated by extraction of a $CHCl_3$ solution of hydrochloride with a water solution of $NaHCO_3$, followed by extraction with NaCl and water. The total yield of the parent amine of **2a** was 27% of white crystals, with a m.p. of 228–230 °C.

^{1}H NMR ($CDCl_3$) δ(ppm): 1.07–1.11 (2H, −CH−$\underline{CH_2}$ equat.); 1.17 (s, 6H, $-CH_3$ equat.); 1.24 (t, 6H, 2 × $\underline{CH_3}$−CH_2−N−, J = 7.14 Hz); 1.31 (s, 6H, $-CH_3$ axial); 2.0 (dd, 2H, −CH−$\underline{CH_2}$ axial); 3.45 (q, 4H, 2 × CH_3−$\underline{CH_2}$−N−, J = 7.12 Hz); 4.36–4.52 (tm, 1H, −CH−); 6.50 (d, 1H, coumarin H-8); 6.65 (dd, 1H, coumarin H-6, J = 8.95 Hz); 7.43 (d, 1H, coumarin H-5, J = 8.96 Hz); 8.64 (d, 1H, −NH−); 8.68 (s, 1H, >C=$\underline{CH}$−methylene).

^{13}C NMR ($CDCl_3$) δ(ppm): 12.4 ($\underline{CH_3}$−CH_2−); 28.5 (CH_3 axial); 34.9 (CH_3 equat.); 42.7 (CH−N); 45.1 ($\underline{CH_2}$−CH−N); 45.2 (CH_3−$\underline{CH_2}$−); 51.1 (C−N); 96.5 (CH-8 coumarin); 108.4 (C-10 coumarin); 109.9 (C-5 naphthalene); 110.4 (C-3 lactone); 131.1 (−CH=methylene); 147.9 (CH-6 coumarin); 152.4 (C-9 coumarin); 157.6 (C-7 coumarin); 162.2 (C=O lactone); 162.7 (C=O amide).

FTIR (KBr) ν (cm^{-1}): 3434, 3315, 2974, 1692, 1648, 1618, 1585, 1537, 1513, 1413, 1355, 1244, 1191, 1136, 798.

Anal. Calcd. for $C_{23}H_{33}N_3O_3$: C69.14, H8.33, N10.52. Found: C68.55, H8.25, N10.25.

2.1.7. 7-(N,N-diethylamino)coumarin-3-carboxy-(1-oxo-2,2,6,6-tetramethylpiperidine-4-yl)amide (**2b**)

The synthesis of **2b** was carried out using a DMT-MM mediator, similar to that of **1b**, using compounds **2** (1.92 mmol), **5** (2.11 mmol) and **7** (2.11 mmol) in THF solution over 18 h. The FTIR analysis of the reaction mixture showed formation of −C=O vibration related to the amide. After the THF evaporation, the residue was dissolved in chloroform, extracted with brine solution and water and dried over anhydrous Na_2SO_4. The product was obtained by chromatographic separation on a SiO_2 column using a $CHCl_3$/MeOH mixture (15/1, v/v) as the first fraction. Yellow-orange crystals of **2b**, with a m.p. of 263–267 °C, were obtained by crystallization from the elution solution during evaporation in 50% yield. The purity of product (98%) was confirmed by ESR analysis comparing with 4-hydroxy-1-oxy-2,2,6,6-tetramethylpiperidine in toluene solution (1×10^{-3} mol L^{-1}).

^{1}H NMR ($CDCl_3$, reduced by pentafluorophenyl hydrazine) δ (ppm): 1.25 (t, 6H, 2 × $\underline{CH_3}$−CH_2−N−); 1.44; (s, 6H, $-CH_3$ equat.); 1.49 (s, 6H, $-CH_3$ axial); 2.04 (t, 2H, −CH−$\underline{CH_2}$ equat.); 2.19 (dd, 2H, −CH−$\underline{CH_2}$ axial); 3.46 (q, 4H, 2 × CH_3−$\underline{CH_2}$−N−); 4.01 (strong singlet, residual from pentafluorophenyl hydrazine); 4.45–4.62 (m, 1H, −CH−); 5.16 (wide, 1H, >N−$\underline{OH}$); 6.50 (d, 1H, coumarin); 6.67 (dd, 1H, coumarin); 7.44 (d, 1H, coumarin); 8.65 (s, 1H, >C=$\underline{CH}$−methylene); 8.82 (d, 1H, −NH−).

FTIR (KBr) ν (cm^{-1}): 3439, 3301, 3040, 2975, 2935, 1706, 1659, 1609, 1565, 1543, 1452, 1362, 1238, 1145, 798, 768, 642.

2.1.8. 7-(N,N-diethylamino)coumarin-3-carboxy-(1-(1′-phenylethyl)oxy-2,2,6,6-tetramethylpiperidine-4-yl)amide (**2c**)

The synthesis of **2c** was carried out using DMT-MM mediator, similar to that of **1c**, using compounds **2** (1.16 mmol), **6** (1.27 mmol) and **7** (1.27 mmol) in THF solution over 48 h. The formed precipitate was separated by filtration and thoroughly washed on the funnel with THF (6 × 10 ml). The solvent was evaporated on a rotary evaporator, and the solid residue was chromatographed on a silica column using gradient elution of *i*-hexane/ethylacetate mixtures, beginning with a 1/1 mixture (v/v) and finishing with a 1/2 mixture (v/v). Orange crystals of **2c** with a m.p. of 230–232 °C were obtained by crystallization from the elution solution during evaporation in 27% yield.

^{1}H NMR ($CDCl_3$) δ(ppm): 0.67 (s, 3H, 1 × CH_3 equat.); 1.17 (s, 3H, 1 × CH_3 equat.); 1.26 (t, 6H, 2 × $\underline{CH_3}$−CH_2−N−); 1.31–1.34

(2 × s, 6H, 2 × $-CH_3$ axial); 1.49 (d, 3H, $-CH-\underline{CH_3}$, $J = 6.69$ Hz); 1.54 (t, 2H, $-CH-\underline{CH_2}$ equat.); 1.79 (td, 1H, $-CH-\underline{CH_2}$ axial); 1.93 (td, 1H, $-CH-CH_2$ axial); 3.45 (q, 4H, 2 × $CH_3-\underline{CH_2}-N-$); 4.29 (m, 1H, $-\underline{CH}-NH-$); 4.79 (q, 1H, $-\underline{CH}-CH_3$, $J = 6.69$ Hz); 6.49 (s, 1H, coumarin); 6.63 (dd, 1H, coumarin); 7.20–7.32 (m, 5H, 1-Phenyl.); 7.415 (d, 1H, coumarin); 8.58 (d, 1H, $-\underline{NH}-CH-$); 8.86 (s, 1H, >C=$\underline{CH}$–methylene).

^{13}C NMR ($CDCl_3$) δ(ppm): 12.6 ($\underline{CH_3}-CH_2-$); 21.1 ($\underline{CH_3}-CH-Ph$); 23.5 (CH_3 axial); 34.1 and 34.8 (CH_3 equat.); 41.4 ($\overline{CH}-N$); 45.3 ($CH_3-\underline{CH_2}-$); 46.3 ($\underline{CH_2}-CH-N$); 60.1 and 60.3 (2 × C–N); 83.4 ($CH_3-\underline{CH}-Ph$); 96.7 (CH-8 coumarin); 108.6 (C-10 coumarin); 110.1 (C-5 coumarin); 110.6 (C-3 lactone); 126.9 (CH-2,6 phenyl); 127.1 (CH-4 phenyl); 128.2 (CH-3,5 phenyl); 131.3 (−CH=methylene); 145.7 (C-1 phenyl); 148.1 (CH-6 coumarin); 152.6 (C-9 coumarin); 157.8 (C-7 coumarin); 162.6 (C=O lactone); 162.9 (C=O amide).

FTIR (KBr) ν (cm^{-1}): 3430, 3313, 2970, 1690, 1647, 1617, 1584, 1536, 1512, 1412, 1354, 1230, 1135, 797, 702.

Anal. Calcd. for $C_{31}H_{41}N_3O_4$: C71.45, H7.95, N8.09. Found: C70.81, H7.85, N7.85.

2.1.9. 7-(N,N-diethylamino)coumarin-3-carboxy-(1-methyl-propyl) amide (**2d**)

The synthesis of **2d** was carried out using a DMT-MM mediator, similar to other derivatives, using **2** (0.46 mmol), *sec*-butylamine **8** (0.85 mmol) and **7** (0.85 mmol) in THF solution over 18 h. The solvent was evaporated on a rotary evaporator from a light yellow reaction solution, and the solid yellow residue was dissolved in chloroform. The organic layer was washed with brine solution (twice) and distilled water (three times) and then dried over anhydrous Na_2SO_4. The product was obtained by chromatographic separation on a SiO_2 column using an *i*-hexane/ethylacetate mixture (1/2, v/v) as the second fraction. A yellow oily residue was identified as the product according to NMR analysis in 40% total yield.

^1H NMR ($CDCl_3$) δ(ppm): 0.96 (t, 3H, $\underline{CH_3}-CH_2-CH-$); 1.21–1.27 (m, 2 × 3H, CH_3-CH- + CH_3-CH_2-N); 1.54–1.64 (d-qui, 2H, $CH_3-\underline{CH_2}-CH-$); 3.45 (q, 4H, 2 × $CH_3-\underline{CH_2}-N-$); 4.07–4.15 (m, 1H, $CH_3-\overline{CH_2}-\underline{CH}-$); 6.52 (s, 1H, coumarin); 6.63 (dd, 1H, coumarin); 7.44 (d, 1H, coumarin); 8.64 (d, 1H, $-\underline{NH}-CH-$); 8.71 (s, 1H, >C=$\underline{CH}$–methylene).

^{13}C NMR ($CDCl_3$) δ(ppm): 10.4 ($\underline{CH_3}-CH_2-CH-$); 12.4 ($\underline{CH_3}-CH_2-N$); 20.4 ($\underline{CH_3}-CH-$); 29.7 ($\overline{CH_3}-\underline{CH_2}-CH-$); 45.0 ($\overline{CH_3}-\underline{CH_2}-$); 46.8 ($CH_3-\overline{CH_2}-\underline{CH}-$); 96.6 (CH-8 coumarin); 108.5 (C-10 coumarin); 109.9 (C-5 coumarin); 110.7 (C-3 lactone); 131.0 (−CH=methylene); 148.0 (CH-6 coumarin); 152.4 (C-9 coumarin); 157.6 (C-7 coumarin); 162.6 (C=O lactone); 162.9 (C=O amide).

FTIR (KBr) ν (cm^{-1}): 3356, 2967, 1686, 1640, 1608, 1584, 1577, 1507, 1456, 1420, 1353, 1260, 1232, 1192, 1136, 1075, 819, 799, 684.

Anal. Calcd. for $C_{18}H_{24}N_2O_3$: C68.33, H7.65, N8.85. Found: C68.55, H7.55, N8.90.

Polymer films doped with dyes were prepared by casting from solution. Films of polystyrene (PS) (Chemische Werke Huels, F.R.G.) and poly(methyl methacrylate) (PMMA) (Diacon, ICI, England) were prepared by the casting of 1 ml of chloroform solution of the polymer (5 g/100 ml) containing the desired amount of dye on a glass plate (28 × 35 mm). The solvent was evaporated slowly. Films of poly (vinylchloride) (PVC) (Neralit, Spolana Neratovice s.e., CR) were prepared in a similar way by casting from tetrahydrofuran solution. The dye concentration in the polymer films was 0.002 mol kg^{-1}.

2.2. Spectral measurements

^1H NMR spectra were recorded in solution on a Bruker AC-300P (300.1 MHz) spectrometer, with the TMS proton signal as an internal standard. FTIR spectra were measured on Nicolet 8700 instrument (Thermo, USA) and ESR spectra on X-band spectrometer E-4 Varian (USA) interfaced with PC using program Symphonia Bruker.

UV-VIS absorption spectra were taken on a spectrometer UV 1650 PC (Shimadzu, Japan).

Fluorescence spectra were recorded on a RF-5301PC spectrofluorophotometer (Shimadzu, Japan) and on a Perkin-Elmer MPF-4 spectrofluorimeter (Perkin-Elmer, Norfolk, Conn. U.S.A.), which was connected through interface and A/D convertors to the ISA slot of a PC using a homemade data collection program. The program Origin 6.1 (Microsoft) was used for data plotting. The fluorescence of the solution was measured in a 1 cm cuvette in the right-angle arrangement. The fluorescence of the polymer films was taken in a front-face arrangement on the solid sample holder.

The quantum yield of the probes (1a–c and 2a–d) in solution and doped in polymer films was determined using anthracene as the standard in the respective medium, taking the quantum yield of anthracene in cyclohexane 0.25 [38]. The quantum yields of anthracene fluorescence in all other media were determined by the comparison of the fluorescence of anthracene in cyclohexane and in respective medium. It was found to be 0.20 in methanol and 0.11 in chloroform. In polymer matrices, the quantum yields were assumed to be 0.20 in PMMA, 0.16 in PS and 0.11 in PVC. The fluorescence spectra were taken using excitation into the maximum of the longest-wavelength absorption band. The anthracene concentration was the same in all media. The quantum yields in solution and in film were corrected for different absorption at the excitation wavelength [39]. The fluorescence spectra were taken by the excitation into the maximum of the longest-wavelength absorption band; the fluorescence spectra of anthracene were excited at 355 nm.

The calculated Φ_{NR}/Φ_{NO} ratio of quantum yields of reduced and oxidized forms of piperidine amine moiety reports the extent of intramolecular quenching or energy transfer from fluorophore to paramagnetic center.

The fluorescence lifetime measurements were performed on a LIF 200 (Lasertechnik Ltd., Berlin, F.R.G.), which operates as a stroboscope. The excitation source is a nitrogen laser emitting at 337 nm, and the emission is selected by a cut-off filter. The output signal of the boxcar integrator was digitized and transferred to the PC using a homemade program. The fluorescence decay curves were evaluated by a simple phase plane method [40] using J. Snyder's program based on [41]. The standard deviation $G^{1/2} = \Sigma((I_{exp} - I_{calc})^2/n)^{1/2}$, where I_{exp} and I_{calc} are the experimental and calculated emission intensity, respectively, is used to judge whether the decay is mono-exponential. The decay curve is assumed to be mono-exponential when $G^{1/2}$ is less than 5%. The fitting of the fluorescence decay curves for a model of bi-exponential decay was performed using the adapted FluoFit MatLab package [42].

The steady-state and time-resolved fluorescence measurements of solutions and polymer films were performed in the presence of air at 1 × 10^{-5} mol L^{-1} concentrations in liquid media and at 0.002 mol kg^{-1} in polymer matrices.

3. Results and discussion

3.1. Synthesis of dyes

7-(*N*,*N*-diethylamino)coumarin-3-carboxylic acid **2** was synthesized by the Knoevenagel condensation of 3-(*N*,*N*-diethylamino)salicylaldehyde with Meldrum's acid, catalyzed with piperidinium acetate in ethanol, according to a known procedure [37].

Esterification or amide formation of acids with directly connected carboxyl groups containing conjugated or aromatic carbohydrates or rings with 4-hydroxy- or 4-amino-2,2,6,6-tetramethylpiperidine derivatives is often problematic due to the lower reactivity of piperidine derivatives. Aromatic acids are also known to have low reactivity, especially for the substitution of aromatic rings with electron-donating substituents. Kunishima et al. [33,34] recently published the synthesis, stability studies and utilization of a triazine-adduct-based ring with *N*-methylmorpholine, originally for low-molecular weight derivatives. The reaction of acids with amines or alcohols mediated with DMT-MM (7) can be performed in commercial, non-dried, tetrahydrofuran solution or directly in water. DMT-MM displays high solubility in water and alcohols without any detectable decomposition. The triazine-based activation of carboxyls is an example of a non-carbodiimide mediator. Currently carbodiimide mediators are often used for such reactions. One of the reported experimental disadvantages of carbodiimides, apart from the high cost, is the contamination of product with stable *N*-acylurea groups or, in the case of 1,3-dicyclohexylcarbodiimide (DCC), the small dissolution of urea and the necessity of dry conditions. On the other hand, triazine-based mediators are frequently used for the activation of the carboxyls of such biopolymers as enzymes, proteins [43] or polysaccharides [35] and synthetic polymers [44].

In the present work, we used **7** for condensation of the coumarin-3-carboxylic acid derivatives **1** and **2** with parent 4-amino-2,2,6,6-tetramethylpiperidine **4**, *N*-oxyl **5** and *N*-alkoxyamine **6** (Schemes 1 and 2). For **1b**, the reaction gave a high product yield. In the cases of **1a** and **2a**, products were achieved in the form of the hydrochloride salt of piperidine because of the higher basicity of the TMP ring compared to *N*-methylmorpholine. Though crude hydrochloride was achieved from the reaction in a high yield (~70%), isolation of the free amine was rather inefficient. In the synthesis of **1c**, the reaction derivative conversion that followed on TLC chromatography was low, and the reaction required increased reaction temperature. However, the yields of pure **1c** and **2c** were lower than 30%. Usually, *N*-alkoxyamine can be prepared in a two-step synthesis by the radical reaction of *N*-oxyl with vinyl (styrene) derivatives and subsequent reduction with $NaBH_4$, as was mentioned here for BOC-NOR and is described in [13,30]. Here, less than 5% yield was obtained for **1c**, together with different side-products, which, according to NMR analysis, did not contain coumarin moieties. As is shown in the Experimental section, such problems were not observed for BOC-protected 4-amino-tetramethylpiperidine-*N*-oxyl (Scheme 3).

3.2. Spectral characterization

3.2.1. Dyes based on coumarin; spectral data in solution and in polymer films

Coumarins **1a**–**c** exhibit absorption bands with fine resolved structures in non-polar cyclohexane at 287, 321 and 329 nm, a shoulder at 295 nm and bands in chloroform and polar methanol centered at 295 and 329 (330) nm without distinguished band at 287 and 321 nm (Table 1). The main emission maxima appear at 307–308 nm in cyclohexane for this type of fluorophore. Emission in chloroform and methanol is redshifted by about 90–100 nm. This shift is quantitatively expressed in large Stokes shift values of over 9500 cm^{-1} in polar methanol and over 9000 cm^{-1} in chloroform in comparison to that in non-polar cyclohexane (about 2300 cm^{-1}). Very low fluorescence intensity, expressed as quantum yield was observed for all coumarin dyes **1a**–**c** in cyclohexane. In MeOH and chloroform, the quantum yields are slightly higher but still low (Table 1). As was reported previously [45] coumarine derivatives substituted by electron-donating groups in position 3 form intramolecular charge-transfer (ICT) or twisted ICT state (TICT). Such dipolar arrangement of molecule with partial positive charge on piperidine amide substituent is effective radiationless route competing with fluorescence. Some comparison with our derivatives **1a**–**c** with carboxyamide group in position 3 could be only speculation. However, large Stokes shift in polar protic methanol is probably a consequence of stabilization of TICT state in this solvent. Bognar et al. [20] reported similar weak fluorescence for this type of fluorophore in polar and aprotic acetonitrile. The intramolecular electron quenching of fluorescence by *N*-oxyl (ratio Φ_{NR}/Φ_{NO}) is practically impossible to determine in cyclohexane due to very low fluorescence intensity; in MeOH and $CHCl_3$, these values lie in the range of 3.0–5.0.

All relevant spectral data for the coumarin-type probe in polymer matrices are given in Table 4. In the absorption spectra of these dyes (parent amine **1a**, *N*-oxyl **1b** and *N*-alkoxy **1c**), there is a broad absorption band at 284–291 nm in PMMA and PS and at 296–299 nm in PVC, with a fairly distinct band or shoulder at around 325–331 nm. This absorption band is not sensitive to the environment. There is no distinct shift in the position of this band or its overall features between the non-polar PS matrix and the more polar PMMA or chlorinated PVC matrices (Fig. 1).

The fluorescence of these dyes is redshifted to 390–400 nm, exhibiting a broad band with a small but distinguished redshifted band at 465 nm, which is visible mainly for **1b**. The Stokes shift is rather large (around 5000 cm^{-1}). The overall fluorescence of the dyes referenced with anthracene under the same conditions is

Table 1
Spectral characteristics of probes based on coumarin and HAS (**1a**–**c**) in solutions at concentration of probes 1×10^{-5} mol L^{-1}.

Dye	Medium	λ_A[a] (log ε) nm	λ_F[b] nm (relative intensity)	$\Delta\nu$[c] cm^{-1}	Φ[d]	Φ_{NR}/Φ_{NO}[e]
1a	cyclohexane	287 (4.09), 295sh, 321, 329	307(1), 327(0.55), 368(0.37)	2331	0.0008	~1.0
1b		287 (4.14), 295sh, 321, 329	308 (1), 334(0.32), 374(0.32)	2315	0.001	–
1c		287 (4.1), 297sh, 321, 328	308 (1), 332(0.36), 370(0.41)	2376	0.001	1.0
1a	MeOH	295 (4.13), 329	393sh, 414	9744	0.02	5.0
1b		295 (4.17), 330	394sh, 409	9564	0.004	–
1c		295 (4.07), 330	393sh, 412	9742	0.015	3.8
1a	$CHCl_3$	295 (4.19), 329	363sh, 386(1), 399(0.99)	8836	0.0056	3.3
1b		295 (4.17) 330	363sh, 385(1), 404(0.99)	9146	0.0017	–
1c		295 (4.18), 330	363sh, 385(1), 404(0.99)	9146	0.0074	4.4

[a] Maxima of the absorption wavelength bands with intensity of the highest wavelength band expressed as log ε.
[b] Maxima of the fluorescence (λ_{exc} = 287 nm in cyclohexane, λ_{exc} = 295 nm in MeOH and $CHCl_3$).
[c] Stokes shift.
[d] Quantum yield of fluorescence based on anthracene.
[e] Extent of intramolecular quenching.

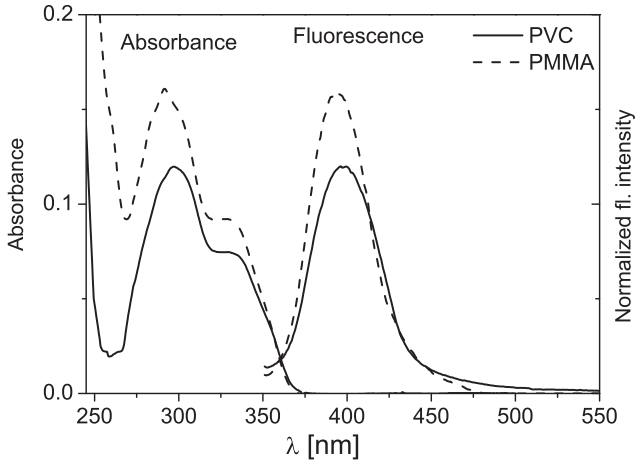

Fig. 1. Absorption and fluorescence spectra of coumarin-3-carboxy-(2,2,6,6-tetramethylpiperidine-4-yl)amide (**1a**) in PVC and in PMMA matrices at 0.002 mol kg^{-1} (excitation wavelength 330 nm).

rather weak, as in liquid media. The absolute quantum yields lie in the range of 0.003–0.05 in all polymer media. The ratio Φ_{NR}/Φ_{NO} reporting the extent of intramolecular quenching is in the range of ~0.64–2.3 and is rather low. Calculated ratio Φ_{NR}/Φ_{NO} with value below 1 for **1a**/**1b** in PMMA matrix is due to low intensity of fluorescence rather than some physical phenomenon. In the polymer matrices, this ratio has a large error, as is demonstrated by the rather wide range of values for the ratio Φ_{NR}/Φ_{NO}, which is 3.5–10 in PS matrix and is listed in Table 4. Therefore, the application of this type of dye for monitoring or imaging radical processes in the solid state and in solutions is rather limited.

3.2.2. Dyes based on diethylamino-coumarin; spectral data in solution and in polymer films

The spectral properties of the coumarin fluorophore with an electron-donating diethylamino group (**2a**–**d**) follow a similar trend as the unsubstituted coumarin **1a**–**c** in terms of used media/matrix but with one significant feature (Tables 2 and 3). The fluorescence intensity is much higher and is accompanied by higher intramolecular quenching, mainly in chloroform. The solubility of tetramethylpiperidine-based dyes in cyclohexane is limited, so only the spectral properties of the alkylamide **2d** model dye are presented.

The absorption bands are redshifted to maxima at 417–420 nm in all liquid media except **2d** in cyclohexane, which exhibits three bands at 381, 392 and 402 nm, indicating some vibrational structure. The emission spectra of the parent amine **2a**, *n*-oxyl **2b**, and *n*-alkoxy amine **2c** exhibit broad bands in range of 446–450 nm in chloroform and 465–467 nm in MeOH (Fig. 2). Comparison with model **2d** shows the slight influence of the tetramethylpiperidine moiety on the spectral properties of the coumarin fluorophore because the absorption and emission maxima of this dye are shifted by 1–4 nm to lower wavelengths in some solvents. Stokes shifts derived from absorption and emission parameters for these type of dyes are much lower, about 1500 cm^{-1} in chloroform and 2200–2400 cm^{-1} in polar solvents for **1a**–**c** (Table 3). Substantially higher quantum yields of such dyes were calculated in chloroform. The intramolecular quenching values in this solvent were more efficient (about 6–7). However, these dyes (**2a**–**c**) exhibit low fluorescence quantum yield and low or negligible intramolecular quenching in polar methanol. This behavior indicates the strong interaction of the protic polar solvent with the electronic excited state of diethylamino-coumarin fluorophore. Comparison with

Table 2
Main spectral parameters of dyes based on diethylamino-coumarin and HAS (**2a**–**d**) in solutions at concentration of probes 1×10^{-5} mol L^{-1}.

Dye	Medium[a]	$\Delta\nu$[b] cm^{-1}	Φ[c]	Φ_{NR}/Φ_{NO}[d]	τ[e] ns
2d	Cy	1620	0.19	–	2.2
2a	MeOH	2397	0.009	1	
2b		2305	0.009	–	
2c		2361	0.0085	1	
2d		2260	0.018	–	1.7
2a	DEG	2152	0.26	0.68	–
2b		2207	0.38	–	–
2c		2207	0.80	2.1	–
2d		2283	0.29	–	–
2a	AcCN	2416	0.14	2.2	–
2b		2404	0.064	–	–
2c		2416	0.15	2.3	–
2d		2427	0.15	–	–
2a	$CHCl_3$	1602	0.41	6.6	2.6
2b		1587	0.062	–	7.6 ps (95%) 2.1 ns (5%)
2c		1502	0.39	6.3	2.5
2d		1509	0.82	–	2.7

[a] Solvent: Cy-cyclohexane, $CHCl_3$-chloroform, DEG-diethylene glycol, AcCN-acetonitril, MeOH-methanol.
[b] Stokes shift.
[c] Quantum yield of fluorescence based on anthracene quantum yields of anthracene in DEG and AcCN were assumed as in methanol (0.2).
[d] Extent of intramolecular quenching.
[e] Lifetime.

spectral data obtained in polar aprotic acetonitrile solution shows slightly different spectral behavior. Quantum yields with more than ten-fold enhancement are observed for all bifunctional dyes and for model **2d** in AcCN. The electron-donating group is one of the components of the entire fluorophore, which could belong to the fluorophore group with a twisted intramolecular charge transfer (TICT) mechanism [46]. Generally, polarity-induced modulation of non-radiative rates (rotation) in polar solvents leads to a decrease of fluorescence intensity. However, the obtained data indicate that hydrogen bonds are eventually responsible for the interaction of the excited carbonyl with not only the amide groups in dyes **2a**–**c** but also the carbonyl of the coumarin lactone ring. The nitrogen atom in the pendant groups may also play some role. To confirm this observation, the spectral characteristics of dyes **2a**–**d** in solvents like toluene and ethylacetate were observed. Data are listed in Table 3. The Lippert–Mataga plot of the fluorescence-maxima wavenumber dependency on the solvent parameter Δf was constructed (Fig. 3). Solvent parameters were calculated according to the following equation:

$$\Delta f = \frac{\varepsilon - 1}{2\varepsilon + 1} - \frac{n^2 - 1}{2n^2 + 1}$$

where ε is the dielectric permittivity, and n is the solvent refractive index [47,48]. The Lippert–Mataga model is useful for fluorescent dyes with an intramolecular charge-transfer states that depend on environment polarity. This simple model is valid for many solvents, with the exception of protic solvents with specific interactions like hydrogen-bonding [48]. The diethylamino-3-carboxy-coumarin fluorophore in dye **2d** does not show strong dependence on solvent polarity because the slope of the linear regression is relatively small in comparison with other typical ICT naphthalene-based dyes like 6-propanoyl-2-(N,N-dimethylamino)naphthalene (PRODAN) or 6-anilino-2-naphthalene sulfonic acid (ANS) [48,49] (Fig. 3B). According to this assumption, protic polar solvents MeOH and DEG should not fit this equation, and points for MeOH and DEG solvents can be omitted from the linear dependency of other solvents. This

Table 3
Absorption, emission maxima and calculated Stokes shifts of **2a**–**d** dyes in different liquid media at concentration of dyes 1×10^{-5} mol L^{-1}.

Medium[a] (Δf)	Parameter	Dye			
		2a	2b	2c	2d
Cy (0.001)	λ_A[b] [nm] (log ε)	–	–	–	381,392,402 (6.59)
	λ_F[c] [nm]	–	–	–	409, 430
	$\Delta\nu$[d] [cm^{-1}]	–	–	–	1620
Toluene (0.013)	λ_A[b] [nm] (log ε)	399sh, 411 (4.60)	398sh, 414 (4.68)	397sh, 412 (4.58)	399sh, 410 (4.51)
	λ_F[c] [nm]	434	439	435	434
	$\Delta\nu$[d] [cm^{-1}]	1289	1376	1283	1349
$CHCl_3$ (0.153)	λ_A[b] [nm] (log ε)	418 (4.75)	420 (4.76)	418 (4.74)	417 (4.59)
	λ_F[c] [nm]	448	450	446	445
	$\Delta\nu$[d] [cm^{-1}]	1602	1587	1502	1509
EtAc (0.201)	λ_A[b] [nm] (log ε)	409 (4.54)	411 (4.46)	410 (4.58)	408 (4.52)
	λ_F[c] [nm]	446	447	446	445
	$\Delta\nu$[d] [cm^{-1}]	2028	1959	1969	2038
DEG (0.266)	λ_A[b] [nm] (log ε)	426 (4.16)	425 (4.02)	425 (3.36)	422 (4.50)
	λ_F[c] [nm]	469	469	469	467
	$\Delta\nu$[d] [cm^{-1}]	2152	2207	2207	2283
AcCN (0.305)	λ_A[b] [nm] (log ε)	414 (4.65)	415 (4.57)	414 (4.50)	413 (4.47)
	λ_F[c] [nm]	460	461	460	459
	$\Delta\nu$[d] [cm^{-1}]	2416	2404	2416	2427
MeOH (0.3093)	λ_A[b] [nm] (log ε)	420 (4.72)	420 (4.37)	419 (4.64)	418 (4.52)
	λ_F[c] [nm]	467	465	465	461
	$\Delta\nu$[d] [cm^{-1}]	2397	2305	2361	2260

[a] Solvent: Cy-cyclohexane, $CHCl_3$-chloroform, EtAc-ethylacetate, DEG-diethylene glycol, AcCN-acetonitril, MeOH-methanol with calculated parameter Δf for construction of Lippert–Mataga plot.
[b] Maxima of the absorption wavelength bands with intensity of the longest-wavelength band expressed as log ε.
[c] Maxima of the fluorescence (λ_{exc} = 420 nm in all media except in cyclohexane).
[d] Stokes shift.

dependency then fits the Lippert–Mataga equation. These results also explain observed low fluorescence intensity in MeOH. The behavior of the bifunctional diethylamino-3-carboxy-coumarin fluorophore linked with a HAS structure in **2a-c** dyes is similar to that of the **2d** dyes (Fig. 3A). A slightly lower dependency was observed for nitroxide **2b** than for the parent amine **2a** and alkoxide **2c**.

The spectral parameters of **2a**–**d** in polymer matrices are listed in Table 4. The absorption and emission spectra of **2c** are shown in Fig. 4. Different polymer matrices do not significantly influence the positions of the absorption and emission maxima of these dyes. However, quantum yields are substantially higher in all polymer matrices (both polar and non-polar) than in liquid media (Tables 2 and 4).

The calculated Φ_{NR}/Φ_{NO} values are also higher (7–12) in polymer matrices. This phenomenon is most likely related to the hindered rotation of diethylamino group in solid matrices. In low-viscosity liquid media, the rotation of this group is free, which leads to the dissipation of excitation energy and the formation of a TICT state. However, in solid polymer matrices, rotations are completely

Table 4
Comparison of the main spectral parameters of fluorophore-HAS dyes **1a**–**c** and **2a**–**c** in polymer matrices at concentration 0.002 mol kg^{-1}.

Medium[a]	Parameter	Dye						
		1a	1b	1c	2a	2b	2c	2d
PS	$\Delta\nu$[b] [cm^{-1}]	8802	8685	8983	2310	2252	2177	2158
	Φ[c]	0.012	0.0032	0.032	0.474	0.026	0.275	0.52
	Φ_{NR}/Φ_{NO}[d]	3.8	–	10	18.2	–	10.6	–
	τ[e] [ns]	–	–	–	2.6	1.1 ps (95%) 1.6 ns (5%)	2.4	2.4
PMMA	$\Delta\nu$[b] [cm^{-1}]	9175	8457	9112	2647	2704	2695	2221
	Φ[c]	0.013	0.008	0.0064	0.42	0.056	0.59	0.42
	Φ_{NR}/Φ_{NO}[d]	1.63	–	0.64	7.5	–	10.5	–
	τ[e] [ns]	–	–	–	3.3	0.1 ps (93%) 2.5 ns (7%)	3.0	3.2
PVC	$\Delta\nu$[b] [cm^{-1}]	8532	8319	8784	2656	2656	2578	2787
	Φ[c]	0.048	0.021	0.032	0.44	0.035	0.304	0.83
	Φ_{NR}/Φ_{NO}[d]	2.3	–	1.5	12.6	–	8.6	–
	τ[e] [ns]	–	–	–	2.8	9 ps (83%) 1.5 ns (17%)	2.8	3.3

[a] Matrix: PS-polystyrene, PMMA-poly(methyl methacrylate), PVC-poly(vinyl chloride).
[b] Stokes shift.
[c] Quantum yield of fluorescence based on anthracene.
[d] Extent of intramolecular quenching.
[e] Lifetime.

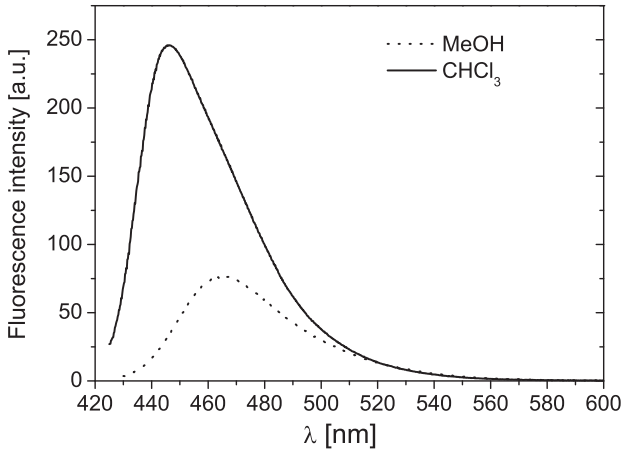

Fig. 2. Comparison of fluorescence spectra of 7-(*N*,*N*-diethylamino)coumarin-3-carboxy-(1-(1′-phenylethyl)oxy-2,2,6,6-tetramethylpiperidine-4-yl)amide (**2c**) in $CHCl_3$ and MeOH solutions at 1×10^{-5} mol L^{-1} (excitation wavelength 420 nm in both media).

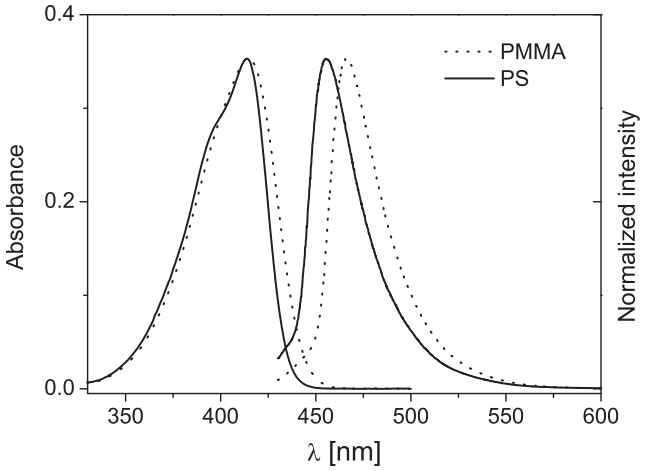

Fig. 4. Absorption and fluorescence spectra of 7-(*N*,*N*-diethylamino)coumarin-3-carboxy-(1-oxo-2,2,6,6-tetramethylpiperidine-4-yl)amide (**2b**) in PS and PMMA polymer matrices at concentration 0.002 mol kg^1 (excitation wavelength 420 nm in both media).

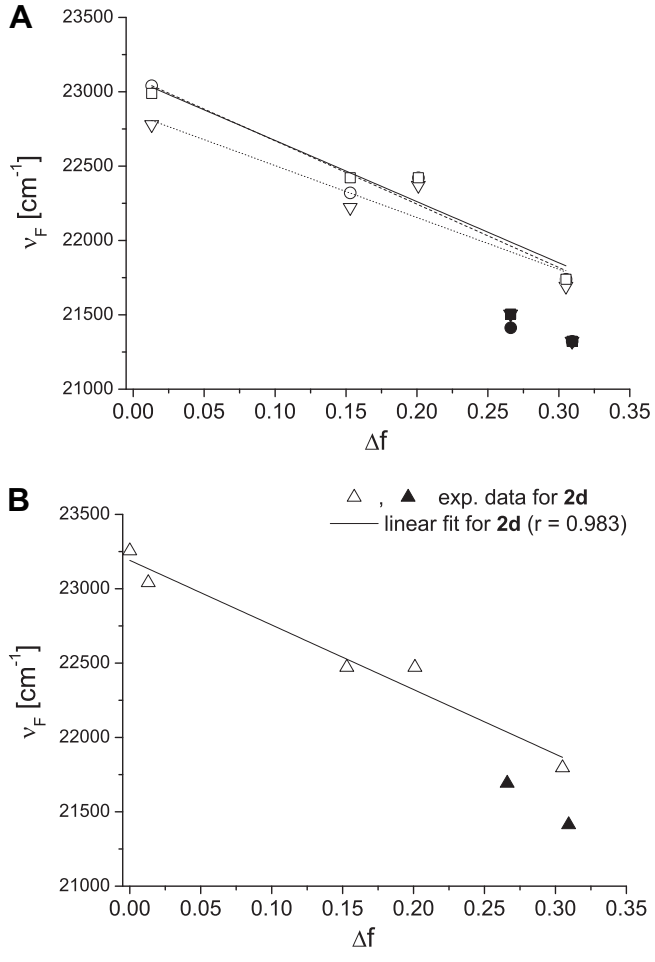

Fig. 3. Lippert–Mataga plots of fluorescence wavenumber maxima of 7-(*N*,*N*-diethylamino)coumarin-3-carboxy-tetramethylpiperidine derivatives **2a**–**c** (A) (2a-rings, linear fit-dashed line; 2b-triangles, linear fit-dotted line; 2c-squers, linear fit-solid line) and model amide **2d** (B) for different solutions. (Solvents and its Δf: cyclohexane (0), toluene (0.013), chloroform (0.153), ethylacetate (0.201), diethylene glycol (0.266), acetonitril (0.305), methanol (0.309)).

hindered. Between these two extremes lie spectral properties in more viscous protic polar diethylene glycol solution (Tables 2 and 4), in which the quantum yield is comparable with values obtained for polymer matrices. These results also suggest that the effect of the hindered rotation of the diethylamino group in DEG is more important for the spectral properties of diethylamino-coumarin fluorophores than the hydrogen-bonding interaction of protic polar solvents.

Concerning the easy conversion of the parent amine of the tetramethylpiperidine moiety to its *N*-oxy radical in the presence of oxygen and the reactivity of this radical with other radical species in photooxidation or thermooxidation processes, these types of bifunctional probes (**2a**–**c** adducts) are applicable as a radical sensor in polymer matrices. However, the 7-diethylamino-3-carboxy coumarin fluorophore can be used alone as a polarity probe in liquid media.

The lifetimes of the excited states of both coumarin-based dye series were short. The lifetimes of dyes **2a**–**d** lie in range of 2–3 ns in chloroform and polymer matrices and are charged with high error (Tables 2 and 4). Our LIF 200 instrument for lifetime measurements is not appropriate to measure short lifetimes below 5 ns. The fluorescence decay profiles of nitroxide **2b** were reasonably fitted by a bi-exponential function. This mathematical expression gives two components with very short lifetimes, in range of picoseconds, with a factor higher than 90% and longer lifetimes in range of nanoseconds. Time-resolved fluorescence measurements in methanol were not successful using our instrument set-up due to the low fluorescence intensity and the solvent interaction with the fluorophore excited state mentioned above. The same problem occurred with the lifetimes of **1a**–**c** dyes as a consequence of its low fluorescence intensity. Fluorescence lifetimes are too short to be quenched by oxygen in diffusion-controlled process.

4. Conclusions

There is a constant search for new, efficient probes that have simple structures, are easy to prepare and exhibit interesting spectral properties distinctly for at least two different spectroscopic states (shining or quenched) for use in monitoring radical oxidation and/or reduction and other processes. Therefore, in this article, we described the detailed synthesis and spectral characterization of

bifunctional fluorescence probes (dyes) with hindered amine piperidine moiety. Simple and easily prepared dyes based on fluorophores, such as coumarin and diethylamino-coumarin, were spectrally characterized in solutions and in solid polymer matrices. Two main parameters, the fluorescence intensity and extent of intramolecular fluorescence quenching by the paramagnetic reaction center of fluorophores, were evaluated and compared with respect to the utilization of these dyes as sensors of radical reactions.

The dyes based on diethylamino-coumarin fluorophore (**2a**–**c**) are promising because their fluorescence is intense and the intramolecular quenching is efficient in non-polar or chlorinated media. Dyes of the coumarin series (**1a**–**c**) generally exhibit very low fluorescence in all liquid media. Observed parameters in polar protic methanol for all dyes are considerably affected by interaction between the protic solvents and the excited state of fluorophores. The viscosity of the environment also plays a role in the spectral parameters of the diethylamino fluorophore through the rotation of the diethylamino group. Therefore, parameters such as fluorescence quantum yield and the intramolecular quenching of dyes are higher in the polymer matrices than in the liquid media. Unfortunately, the overall spectral performance of these dyes in polar media is completely unsatisfactory, and the search for probes for monitoring radical processes in polar media continues.

Acknowledgement

The authors are greatly acknowledged to Grant agency VEGA for financial support through the project 2/0097/09 and Slovak Research and Development Agency through project APVV-0562-07. For NMR measurements provided by the Slovak State Program Project No. 2003SP200280203 are gratefully acknowledged as well. This publication is the result of the project implementation: Center for materials, layers and systems for applications and chemical processes under extreme conditions Stage II supported by the Research & Development Operational Programme funded by the ERDF.

References

[1] Lakowicz JR. Principles of fluorescence spectroscopy. 2nd ed. New York: Kluwer Academia/Plenum Publishers; 1999.
[2] Albani JR. Principles and applications of fluorescence spectroscopy. Oxford, UK: Blackwell Publishing; 2007.
[3] Schnabel W. Polymers and light, fundamentals and technical applications. Wiley-Verlag Chemie GmbH, Weinheim FRG; 2007.
[4] da Silva AP, Gunarante HQN, Gunnlaugsson Th, Huxley AJM, McCoy CP, Rademacher JT, et al. Chem Rev 1997;97:1515–66.
[5] Winnik FM, Regismond STA. Colloids Surf A 1996;118:1–39.
[6] Capek I. Adv Colloid Interface Sci 2002;97:91–149.
[7] Blough NV, Simpson DJ. J Am Chem Soc 1988;110:1915–7.
[8] Gerlock JL, Zacmanidis PJ, Bauer DR, Simpson DJ, Blough NV, Solomon IT. Free Radic Res 1999;10:119–21.
[9] Hrdlovič P, Chmela Š, Búcsiová L. Chem Pap 1996;50:271–8.
[10] Hrdlovič P, Chmela Š. J Photochem Photobiol A 1997;105:83–8.
[11] Búcsiová L, Hrdlovič P, Chmela Š. J Photochem Photobiol A 2001;143:59–68.
[12] Hrdlovič P, Chmela Š, Danko M. J Photochem Photobiol A 1998;112:197–203.
[13] Kollár J, Hrdlovič P, Chmela Š. J Photochem Photobiol A 2008;195:64–71.
[14] Hrdlovič P, Danko M, Chmela Š. J Photochem Photobiol A 2002;149:207–16.
[15] Hrdlovič P, Chmela Š. Polym Degrad Stab 1998;61:177–82.
[16] Búcsiová L, Chmela Š, Hrdlovič P. Polym Degrad Stab 2001;71:135–45.
[17] Danko M, Chmela Š, Hrdlovič P. Polym Degrad Stab 2003;79:333–43.
[18] Kalai T, Hideg E, Vass I, Hideg K. Free Radic Biol Med 1998;24:649–52.
[19] Kalai T, Hankovszky DH, Hideg E, Jeno J, Hideg K, Arkivoc 2002, Part 3, p. 112–120.
[20] Bognár B, Ösz E, Hideg K, Kálai T. J Heterocycl Chem 2006;43:81–6.
[21] Lozinsky E, Martin VV, Berezina TA, Shames AI, Weiss AL, Likhtenshtein GI. J Biochem Biophys Methods 1999;38:29–42.
[22] Yang X-F, Guo X-Q. Anal Chim Acta 2001;434:169–77.
[23] Ortiz RA, Lara AE, Allen NS. Polym Degrad Stab 1999;64:49–54.
[24] Mitcallef AS, Blinco JP, George GA, Reid DA, Rizzardo E, Thang SH, et al. Polym Degrad Stab 2005;89:427–35.
[25] Fairfull-Smith KE, Blinco JP, Keddie DJ, George GA, Bottle SE. Macromolecules 2008;41:1577–80.
[26] Ivan MG, Scaiano JC. Photochem Photobiol 2003;78:416–9.
[27] Coenjarts C, Gracia O, Llauger L, Palfreyman J, Vinette AL, Scaiano JC, et al. Chem Soc 2003;125:620–1.
[28] Scaiano C, Aliaga C, Chretien MN, Frenette M, Focsaneanu KS, Michelsons L'. Pure Appl Chem 2005;77:1009–18.
[29] Bojinov VB. J Photochem Photobiol A 2004;162:207–12.
[30] Danko M, Chmela Š, Hrdlovič P. Polym Degrad Stab 2006;91:1045–51.
[31] Hrdlovič P, Chmela Š, Danko M, Sarakha M, Guyot G. J Fluorescence 2008;18:393–402.
[32] Ma Z, Bobbitt JM. J Org Chem 1991;60:6110–4.
[33] Kunishima M, Kawachi C, Morita J, Terao K, Iwasaki F, Tani S. Tetrahedron 1999;55:13159–70.
[34] Kunishima M, Kawachi C, Iwasaki F, Terao K, Tani S. Tetrahedron Lett 1999;40:5327–30.
[35] Farkaš P, Bystrický S. Carbohydr Polym 2007;68:187–90.
[36] Shendage DM, Froehlich R, Haufe G. Org Lett 2004;6:3675–8.
[37] Song A, Wang X, Lam KS. Tetrahedron Lett 2003;44:1755–8.
[38] Birks JB. Photophysics of aromatic molecules. New York, London, Toronto, Sidney: Willey-Interscience a Division of John Wiley and Sons Ltd; 1968 [Chapter 4], pp. 121–127.
[39] Kawski A, Kubicki A, Kuklinski B, Gryczynski I. J Photochem Photobiol A 1993;71:161–7.
[40] Demas JN, Adamson AW. J Phys Chem 1971;57:2463.
[41] Demas JN. Excited state lifetime measurements. Appendix E. New York: Academic Press; 1973. p. 245.
[42] Enderlein J, Erdmann R. Opt Commun 1997;134:371–8.
[43] Uzagare MC, Sanghvi YS, Salunkhe MM. Synth Commun 2004;34:1071–7.
[44] Thompson K, Michielsen S. J Polym Sci Part A Polym Chem 2006;44:126–36.
[45] Kaholek M, Hrdlovic P. J Photochem Photobiol A 1999;127:45–55.
[46] Rettig W, Lapouyade R. Fluorescence probes based on twisted intramolecular charge transfer (TICT) states and other adiabatic photoreactions. In: Lakowicz JR, editor. Topics in fluorescence spectroscopy. Probe Design and chemical Sensing, vol. 4. New York: Plenum Press; 1994. p. 118–9.
[47] Klymchenko AS, Demchenko AP. Phys Chem Chem Phys 2003;5:461–8.
[48] Lakowicz JR. Principles of fluorescence spectroscopy. 3rd ed. New York: Springer Science+Business Media; 2006 [Chapter 6] Solvent and Environmental Effects, pp. 205–216.
[49] Parusel A. J Chem Soc Faraday Trans 1998;94:2923–7.